Mon. Not. R. Astron. Soc. **000**, 1–8 (2004) Printed 2 February 2008 (MN LATEX style file v2.2)

Molecular fraction limits in damped Lyman-alpha absorption systems

S. J. Curran[1⋆], M. T. Murphy[2], Y. M. Pihlström[3], J. K. Webb[1], A. D. Bolatto[4] and G. C. Bower[4]
[1]*School of Physics, University of New South Wales, Sydney NSW 2052, Australia*
[2]*Institute of Astronomy, Madingley Road, Cambridge CB3 0HA, UK*
[3]*National Radio Astronomy Observatory, Socorro, NM 87801, USA*
[4]*Radio Astronomy Lab, 601 Campbell Hall, University of California, Berkeley, CA 94720, USA*

Accepted —. Received —; in original form —

ABSTRACT
We have used the Green Bank Telescope (GBT) and Berkeley-Illinois-Maryland Association (BIMA) array to search for redshifted millimetre absorption in a sample of damped Lyman-alpha absorption systems (DLAs). This brings the number of published systems searched from 18 to 30. In 17 cases we reach 3σ limits of $\tau \leqslant 0.1$, which is a significant improvement over the previous searches and more than sufficient to detect the 4 known redshifted millimetre absorbers ($\tau \gtrsim 1$). While the CO rotational (millimetre) column density limits obtained are weaker than the electronic (optical) limits, they may provide useful limits below the atmospheric cut-off for the Lyman and Werner H_2-bands in the UV ($z_{\rm abs} \lesssim 1.8$). Using a model for the DLA metallicity evolution combined with assumed HCO^+/H_2 and CO/H_2 conversion ratios, we use the molecular column density limits to calculate plausible H_2 molecular fraction limits. Finally, we use these results to discuss the feasibility of detecting rotational CO transitions in DLAs with the next generation of large radio telescopes.

Key words: quasars: absorption lines–galaxies: ISM–radio continuum: galaxies–cosmology: early universe

1 INTRODUCTION

Molecular absorption lines trace, and provide detailed physical and chemical information about, the cold dense component of the interstellar medium (ISM). Although many detailed studies exist for molecular clouds within our own Galaxy, only relatively recently has detailed information emerged for molecular abundances at high redshift, through absorption studies of redshifted UV molecular hydrogen lines (e.g. Ledoux et al. 2003; Reimers et al. 2003) and millimetre-band rotational lines from molecular tracers (e.g. Wiklind & Combes 1996c).

Observations of a range of different molecular transitions in gas clouds at high redshift would provide a wealth of information on star formation activity in external galaxies, potentially viewed at epochs when chemical abundances and environments were markedly different to today. Such information is invaluable for a detailed understanding of galactic formation and evolution. Furthermore, the narrowness of molecular lines reveals information about small-scale structure in the ISM. Comparison of relative line strengths yields information about the excitation mechanism, and in particular, probes the temperature of the Cosmic Microwave Background (CMB), and hence the expected $(1+z)$–dependence (e.g. Wiklind & Combes 1996c). Finally, comparisons of the relative observed frequencies of millimetre molecular lines (with each other, and/or with atomic transitions arising in the same cloud) can be used to check on any possible variation in certain combinations of the fundamental constants (Drinkwater et al. 1998; Murphy et al. 2001). This last point was the prime motivation for our search for new redshifted millimetre absorbers reported in this paper, although we use the upper limits obtained to yield molecular fraction limits in low redshift DLAs, which is not possible using the UV H_2 lines, which fall below the atmospheric cut-off of $z_{\rm abs} \lesssim 1.8$.

Currently, only 4 redshifted millimetre absorption systems are known (see Wiklind & Combes 1999 and references therein), of which the highest redshift is 0.886 (PKS 1830–211). As a means of approaching a search for new high redshift radio absorbers systematically, we produced a catalogue of DLAs (Curran et al. 2002b)[1], where large column densities ($N_{\rm HI} \geqslant 2 \times 10^{20}$ cm^{-2}) are known to exist, and shortlisted those which are illuminated by radio-loud quasars (i.e. those with a measured radio flux density > 0.1 Jy). This yielded 60 DLAs and sub-DLAs occulting radio-

⋆ E-mail: sjc@phys.unsw.edu.au

[1] A version of this catalogue is kept updated on-line and is available from http://www.phys.unsw.edu.au/∼sjc/dla

loud quasars. Of these, 37 have been searched for 21-cm absorption (see Kanekar Chengalur 2003; Curran et al. 2004b). Selecting those of 12-mm and 3-mm flux densities $\gtrsim 0.1$ Jy, gives 18 systems which have previously been searched for millimetre absorption (Curran et al. 2003), this number now being increased in total to 30 with the observations we present in this paper.

2 OBSERVATIONS AND DATA REDUCTION

2.1 12-mm observations

In Table 1[2] we list all of the known DLAs and sub-DLAs which are illuminated by background sources of $\gtrsim 0.1$ Jy at centimetre wavelengths and have molecular transitions which could be detected in the GBT K-band. In all cases this is both the HCN and HCO^+ $J = 0 \rightarrow 1$ rotational transitions[3]. We chose to observe the latter transition since this tends to be slightly stronger than HCN in the 4 known millimetre absorption systems.

Apart from the sources listed in Table 1, there are only 3 other such DLAs known which have millimetre transitions redshifted to $\approx$ 12-mm: Q 0438–436, RX J1028.6-0844 and LBQS 1213+0922. Although strong ($S \approx 3$ Jy at 12-mm), the first source is far too south to observe with the GBT, and the latter two were estimated to have flux densities too low to yield good optical depth limits within a reasonable integration time. Therefore, using the GBT we hoped for a near complete survey of 12-mm absorption in known DLAs, although due to time constraints we did not observe some of the sub-DLAs (Turnshek et al. 1989; Lanzetta et al. 1991) towards 1017+109, 1021–006 and 1402+044, nor the $N_{\rm HI} = 4\times10^{20}$ cm^{-2} absorber at $z_{\rm abs} = 3.533$ towards 1251–407 (Ellison et al. 2001).

The observations were performed in April 2003, during several consecutive days. Typically, under acceptable observing conditions, the system temperature was 40–100 K. At the time of observing the wide bandwidth spectrometer was unfortunately unavailable and so we used the digital spectral processor with an observing bandwidth of 40 MHz, over 1024 channels. This gave a redshift coverage of $\Delta z_{\rm abs} \approx \pm0.004$, sufficiently wide to cover the absorption redshift uncertainty in most of the DLAs. However, the optical redshifts of 1614+051 and 2131–045 are poorly constrained (Table 1) and so we observed these with five and three overlapping bands, respectively. Dual polarization was used to optimise the sensitivity and beam switching facilitated background emission removal.

The data were reduced using the AIPS++ single dish package and baselines were removed from the spectra by fitting a polynomial function. The continuum levels were measured either during GBT pointing scans of the brightest sources or with the Very Large Array (VLA) in its most compact (D) configuration. These latter data were taken in May 2003, and thus the continuum levels might have altered due to quasar variability, although, as seen from Table 3, these appear to be stable over the 9–11 month period since the ATCA observations. For sources in which no continuum levels were successfully measured within a month of the GBT observations, flux densities were taken or estimated from the literature (see Table 3).

[2] Unless otherwise stated, B1950.0 names are used throughout this paper.
[3] Due to the high dipole moment of the density tracing molecules (i.e. HCN and HCO^+), these will generally be close to the ground state causing the opacity to rival that of the traditional molecular tracer CO which will be excited to higher rotational levels by the CMB at these redshifts.

Table 1. All of the 22 GHz illuminated DLAs and sub-DLAs for which a strong molecular rotational transition falls into the GBT K-band (range 18–26.5 GHz): Prior to the results of Rantakyrö et al. (2004), all of the flux densities were measured or estimated to be $\gtrsim 0.1$ Jy at 12-mm. $N_{\rm HI}$ is the neutral atomic hydrogen column density (cm^{-2}) and $z_{\rm abs}$ is the redshift of the DLA, respectively. $\nu_{\rm obs}$ is the observed frequency of the HCO^+ $0 \rightarrow 1$ line and S is the flux density of the background quasar previously measured at 12-mm.

QSO	$\log_{10} N_{\rm HI}$	$z_{\rm abs}$	$\nu_{\rm obs}$	S
0201+113	21.3	3.38639[7]	20.333	$0.6^{a,d,e}$
0201+365	20.4	2.4614[4]	25.770	0.2*
0335–122	20.8	3.178[9]	21.35	0.14^{e}
0336–017	21.2	3.0619[4]	21.958	0.15^{d}/0.18^{e}
0405–331	20.6	2.570[9]	24.98	0.72^{a}
0528–250	21.2	2.8110[5]	23.403	0.35^{e}
0537–286	20.3	2.974[9]	22.43	1.66^{a}/0.6^{d}/0.9^{e}
0913+003	20.3	2.774[9]	23.82	0.1^{e}
1017+109	19.9	2.380[2]	26.39	0.2*
1021–006	19.6	2.398[2]	26.25	0.15^{c}/0.2^{e}
1251–407	20.6	3.533[9]	19.68	0.06^{e}
...	20.3	3.752[8]	18.77	...
1354–107	20.4	2.501[9]	25.48	0.05^{e}
...	20.8	2.996[8]	22.49	...
1402+044	20.2	2.485[1]	25.59	0.6^{b}
...	20.2	2.688[1]	23.32	...
...	19.9	2.713[1]	24.02	...
1418–064	20.4	3.449[9]	20.05	0.3^{e}
1614+051	20.4	2.52[6]	25.3	GPS
2131–045	20.0	3.27[8]	20.9	$< 0.06^{e}$
2342+342	21.2	2.908[3]	22.82	0.1*

References: (1) Turnshek et al. (1989), (2) Lanzetta et al. (1991), (3) White et al. (1993), (4) Wolfe et al. (1995), (5) Lu et al. (1996), (6) Storrie-Lombardi & Wolfe (2000), (7) Ellison et al. (2001), (8) Péroux et al. (2001), (9) Ellison et al. (2001).
(a) ATCA calibrator, (b) Kovalev et al. (1999), (c) Teräsranta et al. (1998), (d) Curran et al. (2003), (e) Rantakyrö et al. (2004). Note that some flux densities* were estimated from neighbouring frequencies (see Curran et al. 2002b) and that 1614+051 is a Gigahertz Peaked Spectrum source.

Also in May 2003 HCN $0 \rightarrow 1$ at $z_{\rm abs} = 2.713$ towards 1402+044 was observed with the H22 receiver on the Nobeyama 45-m during less than ideal weather conditions during observations for a different (3-mm) project (Curran et al. 2004d). The 250 MHz AOS-W spectrometer (0.25 MHz channels) gave a redshift coverage of $\Delta z_{\rm abs} \approx \pm0.02$.

2.2 3-mm observations

In addition to the GBT survey, follow-up CO observations of candidate molecular absorption detections (Curran et al. 2002a) were carried out using the BIMA array (Table 2). The spectrometer was configured in mode 5, with a central high resolution 100 MHz wide window (0.78 MHz channels) flanked by two lower resolution 200 MHz wide windows (3.125 MHz channels), giving $\Delta z_{\rm abs} \approx \pm0.003 - 0.007$ for $z \sim 0.2 - 2$. Some overlap was added in order to eliminate edge channels and ensure the proper matching of the windows. The antennas where tuned to the redshifted frequency of the chosen CO transition (Lovas 1992), using a redshift that was the average of that of the reported candidate absorption and the corresponding HI absorption ($\Delta z_{\rm abs} \leqslant 0.001$ in all cases). To correct for possible spurious absorption detections due to RF or IF passband features, we interleaved observations of a

Table 2. The BIMA array targets. The parameters are as given in Table 1 where $\nu_{\rm obs}$ is the observed frequency of the CO $0 \rightarrow 1$ line ($2 \rightarrow 3$ for 0458–020) and S is the flux density of the background quasar previously measured at 3-mm.

QSO	$\log N_{\rm HI}$	$z_{\rm abs}$	$\nu_{\rm obs}$	S
0248+430	21.6	0.3939[2]	82.66	0.32^a
0458–020	21.7	2.0399[1]	113.76	$1.4 - 2.6^b$
0738+313	21.3	0.2212[2]	94.39	0.27^a

References: (1) Wolfe et al. (1995), (2) Rao & Turnshek (2000). (*a*) Steppe et al. (1995), (*b*) Tornikoski et al. (2000).

passband calibrator (a strong unresolved radio source) with those of the target quasars every hour. The total integration time on the calibrator is such that the noise introduced by the passband calibration is negligible. Since the data could be self-calibrated, no observations of phase calibrators were performed. The data were reduced using the MIRIAD interferometry reduction package. The visibility cubes were imaged using natural weighting corrected by system temperature, the resulting images were cleaned, and spectra of the central positions were obtained. The final passband-corrected spectra were produced by dividing the spectrum of the source by that of its calibrator, then restoring the continuum level by multiplying by the mean value of the calibrator. The resulting spectra, along with the GBT results, can be viewed at **synergy url here please**

3 RESULTS AND DISCUSSION

3.1 Search results

In Table 3 we show the best previously published optical depths together with our new results, for which, despite the improved limits, there are no absorption features of $\geqslant 3\sigma$ over $\geqslant 3$ km s^{-1}, the full resolution of the BIMA array observations. For all of the limits we estimate the 3σ upper limits on the total column density of each molecule from

$$N_{\rm mm} = \frac{8\pi}{c^3} \frac{\nu^3}{g_{J+1} A_{J+1\rightarrow J}} \frac{Q e^{E_J/kT_x}}{1 - e^{-h\nu/kT_x}} \int \tau dv, \qquad (1)$$

where ν is the rest frequency of the $J \rightarrow J+1$ transition, g_{J+1} and $A_{J+1\rightarrow J}$ are the statistical weight and the Einstein A-coefficient[4] of the transition, respectively, $Q = \sum_{J=0}^{\infty} g_J\ e^{-E_J/kT_x}$ is the partition function[5], for the excitation temperature, T_x, and $\int \tau dv$ is the 3σ upper limit of the velocity integrated optical depth of the line[6].

Since the derived optical depth limits depend upon the r.m.s. noise and thus the velocity resolution (see Curran et al. 2002a), in our previous articles we presented all of the optical depth limits normalised to a spectral resolution of 1 km s^{-1}, the finest resolution typical of most current wide-band spectrometers. Previously, we also quoted column density upper limits per unit km s^{-1} line-width. However, in order to use our limits to constrain molecular fractions at low redshift (Section 3.2), we shall now adopt a line-width (FWHM) of 10 km s^{-1}, which is close to those of the 4 known systems (e.g. Wiklind & Combes 1996c). This is done for a resolution of the same value and so the column density limits, which are calculated for an excitation temperature[7] of 10 K at $z_{\rm abs} = 0$, represent a one channel 3σ detection of a 10 km s^{-1} wide line.

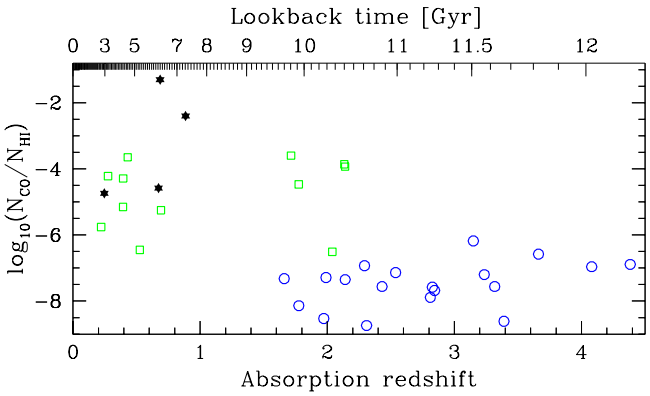

Figure 1. The normalised CO column density versus the absorption redshift. The unfilled markers designate upper limits – squares for the millimetre searches and circles for the optical searches. The filled stars represent the 4 known millimetre absorption systems. The lookback time is for $\Omega_{\rm m} = 0.30, \Omega_\Lambda = 0.70, H_0 = 70\,{\rm km\,s^{-1}\,Mpc^{-1}}$.

3.2 Deriving molecular fraction limits

Despite our improved limits there has yet to be a detection of a rotational molecular transition in a DLA. In many cases the limits far exceed those required to detect the 4 known redshifted millimetre absorbers (see below, Figs. 1 and 2). These systems have molecular fractions of $f \equiv \frac{2N_{\rm H_2}}{2N_{\rm H_2}+N_{\rm HI}} \approx 0.3 - 1.0$ (e.g. Combes & Wiklind 1998), c.f. $f \sim 10^{-7} - 10^{-2}$ for the 10 DLAs in which molecular hydrogen has been detected at UV and optical wavelengths (Reimers et al. 2003 and references therein). In this section we investigate the possibility of detecting molecular tracers in systems with such low molecular fraction.

In Fig. 1 we show the CO rotational (Table 3) and electronic (Ge et al. 1997; Lu et al. 1999; Petitjean et al. 2002) column density limits along with the values for the 4 known systems. While this illustrates the sensitivity to detecting absorption in the known systems, it clearly shows that the radio searches are considerably less sensitive than the optical CO searches[8]. They do, however, complement the optical results in giving limits at redshifts of $z_{\rm abs} \lesssim 1.8$ (below the atmospheric cut-off for direct optical H_2 detections). In Fig. 2 we show the HCO^+ column density limits. Again we see that our limits are more than sufficient to detect HCO^+ in the 4 known systems (Wiklind & Combes 1995, 1996a,b, 1997), with two cases having been searched to at least an order of magnitude better than that required to detect the known systems at low redshift.

[4] These are taken from Chandra et al. (1995, 1996) or derived from the dipole moment (e.g. Rohlfs & Wilson 2000).

[5] The energy of each level, E_J, is obtained from the JPL Spectral Line Catalog (Pickett et al. 1998).

[6] $\int \tau dv \approx 1.06\,\tau_{\rm mm} \times$ FWHM for a Gaussian profile, where $\tau_{\rm mm}$ is the 3σ peak optical depth limit (Table 3).

[7] Due to the increase of CMB temperature with redshift, $T_{\rm CMB} = 2.73(1 + z_{\rm abs})$, T_x increases to 20 K at $z_{\rm abs} = 3.75$, the highest redshift of our sample. The main effect of this is to increase the HCO^+ $0 \rightarrow 1$ column density estimates by a factor of $\leqslant 4$ in comparison to a constant value of 10 K.

[8] Although the deep integrations of 0235+164 and 0458–020 with the NRO 45-m telescope (Takahara et al. 1987; Tsuboi & Nakai 1991) do approach the optical limits.

Table 3. Summary of published searches for molecular tracer absorption in DLAs and sub-DLAs. $\nu_{\rm obs}$ is the approximate observed frequency (GHz), V is the visual magnitude of the background quasar and S is the flux density (Jy) at $\nu_{\rm obs}$ which, unless flagged, is the value obtained during the actual observations (the limits are 1σ and blanks in this field indicate that no value is given in the literature). $N_{\rm HI}$ (cm^{-2}) is the DLA column density from the Lyman-alpha line and $\tau_{21\ {\rm cm}}$ is the normalised peak optical depth of the redshifted 21-cm line (see Curran et al. 2004b for details). The optical depth of the relevant millimetre line is calculated from $\tau = -\ln(1-3\sigma_{\rm rms}/S)$, where $\sigma_{\rm rms}$ is the r.m.s. noise level. Since $\sigma_{\rm rms}$ is dependent on the spectral resolution, we take the various published values and recalculate $\sigma_{\rm rms}$ at a resolution of 10 km s^{-1} ($\tau_{\rm mm}$) and quote only the best existing limit. For all optical depths, 3σ upper limits are quoted and "–" designates where $3\sigma > S_{\rm cont}$, thus not giving a meaningful value for this limit. The penultimate column gives the corresponding column density (cm^{-2}) per 10 km s^{-1} channel (see main text).

DLA	$z_{\rm abs}$	Transition	$\nu_{\rm obs}$	V	S	$N_{\rm HI}$	$\tau_{21\ {\rm cm}}$	$\tau_{\rm mm}$	$N_{\rm mm}$	Ref.
0201+113	3.38639	HCO$^+$ 0 $\rightarrow$ 1	20.3	19.5	0.47	2×10^{21}	$\leqslant 0.09$	<0.007	$<1\times10^{12}$	10
0201+365	2.4614	HCO$^+$ 0 $\rightarrow$ 1	25.8	17.9	0.09^V	3×10^{20}		<0.1	$<1\times10^{13}$	10
0235+164	0.52400	CO 0 $\rightarrow$ 1	75.6	15.5	2.5	4×10^{21}	0.64	<0.02	$<1\times10^{15}$	2
...	0.52398	CO 1 $\rightarrow$ 2	151.3	...	1.27	...	...	<0.03	$<1\times10^{15}$	6
...	...	HCO$^+$ 3 $\rightarrow$ 4	234.1	...	0.75	...	...	<0.1	$<7\times10^{12}$	6
...	0.523869	CS 2 $\rightarrow$ 3	96.4	...	1.7	...	...	<0.1	$<4\times10^{13}$	8
0248+430	0.3939	CS 2 $\rightarrow$ 3	105.4	17.7	<0.2	4×10^{21}	0.2	<0.4	$<1\times10^{14}$	8
...	0.394	CO 0 $\rightarrow$ 1	82.7	...	0.21	...	...	<0.4	$<3\times10^{16}$	10
0335–122	3.178	HCO$^+$ 0 $\rightarrow$ 1	21.4	20.2	$0.13^{A,V}$	6×10^{20}	<0.008	<0.03	$<6\times10^{12}$	10
0336–017	3.0619	HCO$^+$ 0 $\rightarrow$ 1	22.0	18.8	0.15^A	2×10^{21}	<0.007	<0.03	$<5\times10^{12}$	10
0405–331	2.570	HCO$^+$ 0 $\rightarrow$ 1	25.0	19.0	0.53	4×10^{20}		<0.02	$<3\times10^{12}$	10
0458–020	2.0397	HCO$^+$ 2 $\rightarrow$ 3	88.0	18.4		5×10^{21}	0.3	<0.3	$<1\times10^{13}$	7
...	2.0399	...	88.0	...	1.3	...	...	<0.07	$<3\times10^{12}$	8
...	2.03937	CO 0 $\rightarrow$ 1	37.9	...	≈ 0.8	...	...	<0.01	$<1\times10^{15}$	4
...	2.0398	CO 2 $\rightarrow$ 3	113.8	...	0.53	...	...	<0.1	$<6\times10^{15}$	10
...	2.0397	CO 2 $\rightarrow$ 3	113.8	...	0.53^a	...	...	<0.6	$<4\times10^{16}$	5
...	2.0399	CO 3 $\rightarrow$ 4	151.7	...	0.4	...	...	<0.4	$<4\times10^{16}$	8
...	2.04	H_2CO $1_{10}\rightarrow1_{11}$	1.6	...		...	...	<0.01		3
0528–2505	2.1408	CO 2 $\rightarrow$ 3	110.1	19.0	$\approx 0.2^b$	4×10^{20}	<0.3	<1.0	$<6\times10^{16}$	5
...	...	HCO$^+$ 0 $\rightarrow$ 1	23.4	...	$0.3^{A,V}$	...	...	<0.02	$<3\times10^{12}$	10
0537–286	2.974	HCO$^+$ 0 $\rightarrow$ 1	22.4	19.0	0.58	2×10^{20}	<0.007	<0.02	$<3\times10^{12}$	9
0738+313	0.2212	CO 0 $\rightarrow$ 1	94.4	16.1	0.48	2×10^{21}	≈ 0.07	<0.04	$<3\times10^{15}$	10
0827+243	0.5247	CS 2 $\rightarrow$ 3	96.4	17.3	2.7	2×10^{20}	0.007	<0.09	$<3\times10^{13}$	8
08279+5255	2.97364	HCO$^+$ 0 $\rightarrow$ 1	44.9	15.2		1×10^{20}		*No 7 mm flux available*		8
...	...	CO 2 $\rightarrow$ 3	87.0	...	<0.1	...	...			8
0834–201	1.715	HCO$^+$ 2 $\rightarrow$ 3	98.6	18.5	1.7	3×10^{20}		<0.1	$<4\times10^{12}$	8
...	...	HCO$^+$ 3 $\rightarrow$ 4	131.4	...		...	...	<0.2	$<1\times10^{13}$	7
...	...	CO 3 $\rightarrow$ 4	169.8	...	0.9	...	...	<0.7	$<8\times10^{16}$	8
0913+003	2.774	HCO$^+$ 0 $\rightarrow$ 1	23.8	–	$\approx 0.17^{A,V}$	2×10^{20}		<0.04	$<6\times10^{12}$	10
1017+1055	2.380	CS 2 $\rightarrow$ 3	43.5	17.2		8×10^{19}		*No 7 mm flux available*		8
...	...	CO 2 $\rightarrow$ 3	102.3	...	<0.2	...	...	–	–	8
1215+333	1.9984	CO 2 $\rightarrow$ 3	115.3	18.1		1×10^{21}		*No 3 mm flux available*		5
1229–021	0.3950	CO 0 $\rightarrow$ 1	82.6	16.8	0.2	1×10^{21}	0.05	<0.7	$<5\times10^{16}$	8
...	...	CO 1 $\rightarrow$ 2	165.3	...	<0.1	...	...	–	–	8
...	0.39498	CO 1 $\rightarrow$ 2	165.3	...	0.11	...	...	–	–	6
1251–407	3.752	HCO$^+$ 0 $\rightarrow$ 1	18.8	23.7	$\approx 0.1^{A,V}$	2×10^{20}		<0.09	$<2\times10^{13}$	10
1328+307	0.69215	HCO$^+$ 1 $\rightarrow$ 2	105.4	17.3	0.50	2×10^{21}	0.02	<0.2	$<6\times10^{12}$	6
...	...	CS 2 $\rightarrow$ 3	86.9	...	1.0	...	....	<0.3	$<8\times10^{13}$	8
...	...	CO 1 $\rightarrow$ 2	136.2	...	0.39	...	...	<0.3	$<1\times10^{16}$	6
...	...	CO 2 $\rightarrow$ 3	204.4	...	0.27	...	...	<0.5	$<3\times10^{16}$	6
1331+170	1.7764	CO 0 $\rightarrow$ 1	41.5	16.7	0.5	3×10^{21}	0.02	<0.4	$<5\times10^{16}$	1
...	1.7755	...	41.5	...	...	...	...	<0.4	$<5\times10^{16}$	1
1354–107	2.501	HCO$^+$ 0 $\rightarrow$ 1	25.5	19.2	$\approx 0.07^{A,V}$	3×10^{20}	<0.015	<0.08	$<1\times10^{13}$	10
...	2.996	...	22.5	...	...	...	...	<0.1	$<2\times10^{13}$	10
1402+044	2.713	HCO$^+$ 0 $\rightarrow$ 1	24.0	19.8	0.21^*	8×10^{19}		<0.008	$<1\times10^{12}$	10
...	...	HCN 0 $\rightarrow$ 1	23.9	...	0.6	...	...	<0.02	$<8\times10^{12}$	10
1418–064	3.449	HCO$^+$ 0 $\rightarrow$ 1	20.1	18.5	0.14	3×10^{20}		<0.02	$<4\times10^{12}$	10
1451–375	0.2761	HCO$^+$ 1 $\rightarrow$ 2	139.8	16.7	0.6	1×10^{20}	<0.007	<0.2	$<7\times10^{12}$	8
...	...	CO 0 $\rightarrow$ 1	90.3	...	1.2	...	...	<0.1	$<8\times10^{15}$	8

References: (1) Takahara et al. (1984), (2) Takahara et al. (1987), (3) Briggs et al. (1989), (4) Tsuboi & Nakai (1991), (5) Wiklind & Combes (1994), (6) Wiklind & Combes (1995), (7) Wiklind & Combes (1996b), (8) Curran et al. (2002a), (9) Curran et al. (2003), (10) This paper.
Flux densities: ^{A}ATCA June & August 2002 (Curran et al. 2003; Rantakyrö et al. 2004), ^{V}VLA May 2003. Where the flux densities could not be obtained from the data/article – ^{a}the BIMA array value, ^{b}interpolated between 11 GHz and K-band, ^{c}interpolated between radio and 0.5–10 keV, ^{d}extrapolated from 0.4 and 5 GHz. *This observation of 1402+044 is from preliminary (February 2003) GBT observations using the wide band spectrometer.

Table 3. *Continued*

DLA	$z_{\rm abs}$	Transition	$\nu_{\rm obs}$	V	S	$N_{\rm HI}$	$\tau_{21\ {\rm cm}}$	$\tau_{\rm mm}$	$N_{\rm mm}$	Ref.
1614+051	2.52	HCO^+ $0 \rightarrow 1$	25.3	19.5	$\sim 0.3^c$	3×10^{20}		< 0.03	$< 4 \times 10^{12}$	10
2131–045	3.27	HCO^+ $0 \rightarrow 1$	20.9	20.0	$< 0.06^A$	1×10^{20}		–	–	10
2128–123	0.4298	CS $2 \rightarrow 3$	102.8	15.5	0.75	2×10^{19}	< 0.003	< 0.04	$< 1 \times 10^{13}$	7
...	...	CS $3 \rightarrow 4$	137.1	...	0.70	...	...	< 0.05	$< 2 \times 10^{13}$	7
...	...	CO $1 \rightarrow 2$	161.2	...	0.5	...	...	< 0.2	$< 6 \times 10^{15}$	7
...	...	CO $2 \rightarrow 3$	241.9	...	0.4	...	...	< 0.2	$< 1 \times 10^{16}$	7
2136+141	2.1346	HCO^+ $2 \rightarrow 3$	85.4	18.9	0.59	6×10^{19}		< 0.1	$< 4 \times 10^{12}$	6
...	...	CO $2 \rightarrow 3$	110.3	...	0.27	...	...	< 0.2	$< 9 \times 10^{15}$	7
...	...	CO $3 \rightarrow 4$	147.1	...	0.21	...	...	< 0.2	$< 2 \times 10^{16}$	7
...	...	CO $5 \rightarrow 6$	220.6	...	0.16	...	...	< 0.6	$< 8 \times 10^{17}$	7
2342+342	2.908	HCO^+ $0 \rightarrow 1$	22.8	18.4	$\sim 0.1^d$	2×10^{21}	< 0.03	< 0.04	$< 7 \times 10^{12}$	10

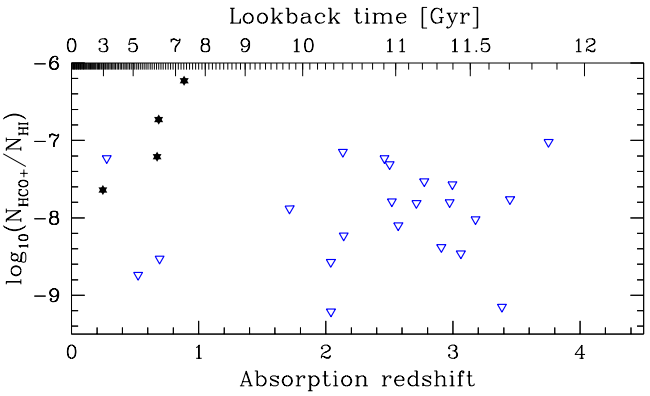

Figure 2. The normalised HCO^+ column density versus the absorption redshift. Again the stars represent the 4 known systems and the inverted triangles are the DLA upper limits (Table 3).

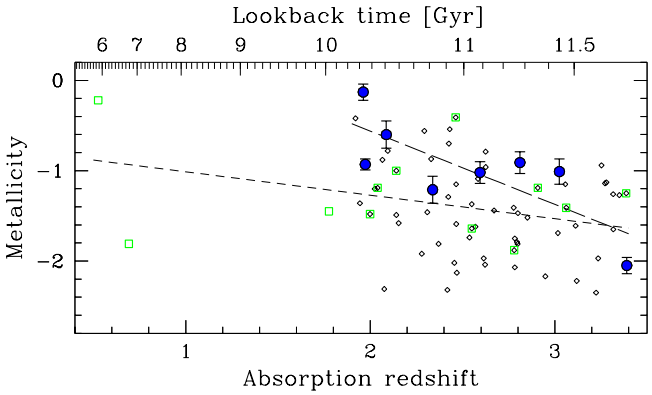

Figure 3. The metallicity evolution of DLAs. The filled circles represent the DLAs which exhibit H_2 absorption with the least-squares fit shown (Curran et al. 2004c), the small unfilled diamonds represent the metallicity measurements of 60 DLAs between $1.9 < z_{\rm abs} < 3.4$ (i.e. the general population), again with the fit shown (Prochaska et al. 2003), and the unfilled squares are the DLAs searched for millimetre absorption (Table 3).

Although we cannot match the sensitivity to molecular absorption provided by the optical results, we can nevertheless attempt to derive constraints on the molecular fraction for absorption systems at low redshift. The major obstacle in this is determining which $N_{\rm CO}$–$N_{\rm H_2}$ conversion ratio to apply: Unlike HCO^+ (discussed later), the ratio may vary from $N_{\rm H_2} \sim 10^6 N_{\rm CO}$ for diffuse gas (Liszt & Lucas 2000a) to $N_{\rm H_2} \sim 10^4 N_{\rm CO}$ for dense, dark Galactic clouds. This latter value is applied to the 4 known millimetre absorbers to yield molecular fractions from rotational lines (see Wiklind & Combes 1998)[9]. However, DLAs have lower metallicities than Galactic systems and are less visually obscured than the 4 known systems, thus casting doubt on whether applying this conversion ratio is justified.

If we extrapolate the metallicity ([M/H][10]) evolution of the general DLA population[11] according to $[{\rm M/H}] \approx -0.26 z_{\rm abs}$ (Kulkarni & Fall 2002; Prochaska et al. 2003), we obtain $[{\rm M/H}] \approx -0.75$ at $z_{\rm abs} \sim 0$ (Fig. 3). At zero redshift this is still significantly lower than solar values suggesting that, in addition to lower enrichment at high redshift, there may be appreciable dust depletion of the metals, as in dense Galactic clouds (e.g. Savage & Sembach 1996), although this may be more relevant to the H_2-bearing DLAs where $f \gtrsim 10^{-2}$ at $z_{\rm abs} \lesssim 1.8$ (Curran et al. 2004c). Moreover, Ledoux et al. (2003) suggest that the large depletion factors in DLAs indicate a significant dust content. Therefore, a fair compromise between the diffuse/dark cases may be to assume the conversion ratio for dark clouds but scaled by the abundance of metals from which the tracer molecules form, i.e. $N_{\rm H_2} \approx 10^{4.75} N_{\rm CO}$ at $z_{\rm abs} \sim 0$. Since the metallicity decreases with increasing redshift, we may expect the conversion of tracer to molecular hydrogen column density to scale accordingly. We therefore apply the ratio of $N_{\rm H_2} \approx 10^{0.26 z_{\rm abs} + 4.75} N_{\rm CO}$, based upon the metallicity evolution of the general DLA population[12]. This gives $N_{\rm H_2} \sim 10^5 N_{\rm CO}$ at $z \sim 1$ rising to $N_{\rm H_2} \sim 10^6 N_{\rm CO}$ at $z \sim 5$. From optical CO limits, Black et al. (1987) and Chaffee et al. (1988) have previously noted

[9] Since all of these sources absorb at low redshift, $z_{\rm abs} \leqslant 0.87$, and have $V \gtrsim 20$ there is currently little chance of detecting the H_2 line directly.

[10] Defined as the heavy element abundance with respect to hydrogen, relative to that of the solar neighbourhood: $[{\rm M/H}] \equiv \log_{10}[N({\rm M})/N({\rm H})] - \log_{10}[N({\rm M})/N({\rm H})]_\odot$.

[11] Due to many of the sources in Table 3 having low redshifts and/or high visual magnitudes, there are only metallicity measurements for half of these sources, all of which belong to the sample of Prochaska et al. (2003). Therefore, by definition these follow the same metallicity evolution of the general DLA population rather than that of the H_2-bearing DLAs (Curran et al. 2004c).

[12] Since the molecular hydrogen fraction shows a strong anti-correlation with redshift for the H_2-bearing DLAs (Curran et al. 2004c and Fig. 4), we may expect less depletion and thus relatively higher metallicities. Fig. 3 does appear to suggest, however, that the metallicity is dominated by poorer chemical enrichment at higher redshifts.

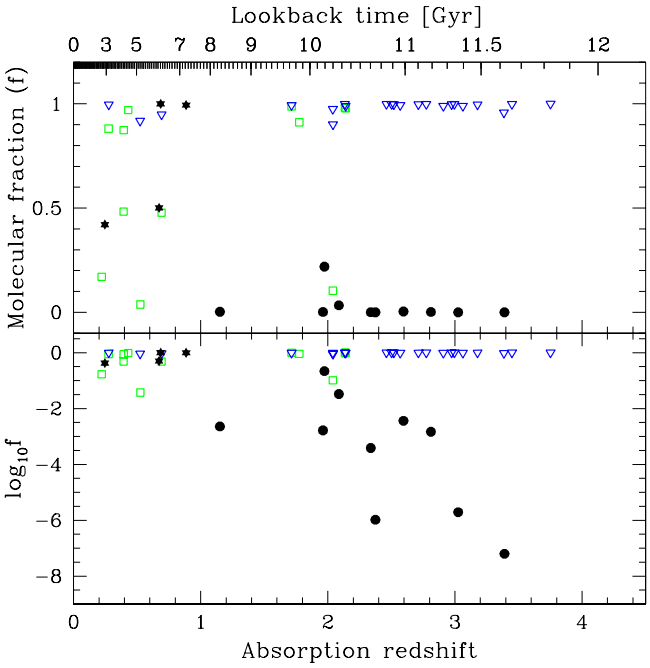

Figure 4. Molecular fractions measured in redshifted absorbers. Again the unfilled symbols represent the upper limits from the millimetre searches, $N_{\rm H_2} = 10^{4.75} N_{\rm CO}$ and $T_x = 10$ K at $z_{\rm abs} = 0$, with the squares representing CO and the inverted triangles HCO^+. The circles represent the H_2-bearing DLAs and the stars the 4 known millimetre absorption systems ($N_{\rm H_2} = 10^4 N_{\rm CO}$ and $T_x = 10$ K, $\forall z_{\rm abs}$). A log version of the plot is also shown by means of a detail of the H_2-bearing systems. This clearly illustrates the evolution of f described by Curran et al. (2004c).

that the carbon to hydrogen column density ratio is a tenth of the Galactic value at $z_{\rm abs} = 1.7$ and 2.3.

In addition to CO, we can use the HCO^+ limits, which could be a better choice of tracer, since a near constant ratio of $N_{\rm HCO^+} = 2 - 3 \times 10^{-9} N_{\rm H_2}$ is found over various regimes in the Galaxy (Liszt & Lucas 2000b). Applying the conversion thus suggests that $N_{\rm H_2} \sim 10^9 \rightarrow 10^{10} N_{\rm HCO^+}$ at $z \sim 1 \rightarrow 5$, i.e. $N_{\rm H_2} \approx 10^{0.26 z_{\rm abs} + 9.34} N_{\rm HCO^+}$. In Fig. 4 we show the derived molecular fractions of the CO and HCO^+ limits together with those of the H_2-bearing DLAs[13]. From this we see that the high conversion ratio and excitation above the $0 \rightarrow 1$ transition make the HCO^+ molecule insensitive with current telescopes to $f \lesssim 1$: Although in many cases our GBT observations yield significantly better limits than previously (Table 3), these are all at high redshift and therefore convert less favourably to molecular fractions due to the steep metallicity evolution. Thus, we obtain near constant limits to the fraction across the entire redshift range searched for HCO^+. Note that the optical CO limits (Fig. 1) occupy the space between the HCO^+ limits and the H_2-bearing DLAs ($1.7 \lesssim z_{\rm abs} \lesssim 4.4$, $-3 \lesssim \log_{10} f \lesssim -0.5$) when the conversion is applied.

We do see however, based on our redshift dependent conversion factor, that the millimetre CO searches generally give interesting (low redshift) limits, with two of the limits within the range of the H_2-bearing DLAs. This suggests that, were these DLAs H_2-bearing[14], making the $N_{\rm CO}$–$N_{\rm H_2}$ conversion reasonable, the CO rotational transition could have been detected in these DLAs: 0235+164 ($z_{\rm abs} = 0.524$) and 0738+313 ($z_{\rm abs} = 0.221$). Unfortunately, there are no metallicity measurements available for these, although (Prochaska et al. 2003) use the value of $[{\rm M/H}] = -0.22 \pm 0.15$ for 0235+164 which comes from model dependent X-ray measurements (Turnshek et al. 2003). Several other models give lower values than this, thus suggesting that this DLA may belong to the general population ($[{\rm M/H}] \approx -0.9$), although the value quoted by Prochaska et al. (2003) could place it in either population (Fig. 3). The general population fit is, however, consistent with the range of $-1.4 < [{\rm M/H}] < -0.4$ at $z_{\rm abs} \approx 0.4$ estimated by Turnshek et al. (2003) and the fact that we did not detect CO. Regarding the molecular fraction, the data are sensitive to $\log_{10} f \sim -1.5$ for the general population metallicity and $\log_{10} f \sim -2.1$ for the value used by Prochaska et al. (2003). This latter fraction shifts this DLA further into the H_2-bearing DLA regime.

For more diffuse clouds of low dust content our limits become weaker with $f \geqslant 0.4$, c.f. $\geqslant 0.03$ previously, being obtained for $N_{\rm H_2} \sim 10^6 N_{\rm CO}$ and $T_x = 10$ K at $z_{\rm abs} = 0$, although in the diffuse gas case the column density limits would improve slightly due to lower excitation temperatures (at best a factor of ≈ 0.5 lower than given in Table 3)[13]. That is, the clouds being diffuse could also explain why no millimetre absorption of CO was detected.

3.3 Detecting millimetre lines in DLAs with the next generation of large radio telescopes

Applying the conversion of tracer column densities described above, we can ascertain the likelihood of detecting these molecular tracers in DLAs with the next generation of large radio telescopes. For $N_{\rm H_2} = 10^{4.75} N_{\rm CO}$ and $T_x = 10$ K at $z_{\rm abs} = 0$:

(i) The Atacama Large Millimeter Array (ALMA)[15]: The 3-mm band of this telescope will give CO $0 \rightarrow 1$ coverage to $z \leqslant 0.34$. At 10 km s^{-1} resolution, one hour of integration will give an r.m.s. of ≈ 0.3 mJy. For a 0.3 Jy continuum flux (fairly typical in Table 3), this corresponds to a 3σ column density limit of $N_{\rm CO} \sim 10^{14}$ cm^{-2} per channel. Applying the conversion at these redshifts gives $N_{\rm H_2} \sim 10^{19}$ cm^{-2} thus giving $f \sim 10^{-3} - 0.1$ for DLAs. If we extrapolate the molecular fractions in H_2-bearing systems back to $z \lesssim 0.3$ (Fig. 4), we see that such limits could well be sufficient to detect rotational CO in DLAs at low redshift.

(ii) The Square Kilometre Array (SKA)[16]: With a tuning range of 0.15 to 20 GHz this telescope can observe CO at $z \geqslant 4.8$. With the same parameters as above, an r.m.s. of 5 μJy is reached giving $N_{\rm CO} \sim 10^{12}$ cm^{-2} per channel[17], thus rivalling current optical limits. At $z \sim 5$, $N_{\rm H_2} \sim 10^6 N_{\rm CO}$ giving $f \sim 10^{-4} - 10^{-2}$ for DLAs, i.e. the molecular fraction range of 7 of the 10 H_2-bearing DLAs (e.g. Reimers et al. 2003). Unfortunately at $z \gtrsim 5$, extrapolating the molecular fraction–redshift anti-correlation, we expect $f \lesssim 10^{-12}$, thus making it unlikely that redshifted millimetre tran-

[13] Versions of Fig. 4 for $N_{\rm H_2} = 10^6 N_{\rm CO}$ and $10^4 N_{\rm CO}$ can be viewed at **synergy url here please**

[14] H_2 is detected in $\lesssim 20\%$ of recent DLA surveys (Ledoux et al. 2003), and so we perhaps expect a $\approx 1/5$ chance of having observed an H_2-bearing system.

[15] http://www.eso.org/projects/alma/

[16] http://www.skatelescope.org/

[17] Again, this is for a flux density of 0.3 Jy. Due to the antenna temperature dominating the system at these low frequencies, an increased flux does not improve the optical depth to the same extent as for the millimetre observations. Therefore, the column density estimate is fairly robust.

sitions could be detected[18] with the SKA, despite its superior sensitivity[19].

4 SUMMARY

We have used the GBT and BIMA array to search for HCO^+ and CO absorption in 19 damped Lyman-alpha absorption systems. Although in many cases the sensitivity reached far surpasses that required to detect the 4 known redshifted millimetre absorption systems, a rotational millimetre-band transition has yet to be detected in a DLA. From optical studies it is revealed that molecular fractions in DLAs are much lower than those of the 4 known systems and, in those where H_2 has been detected, the H_2 molecular fraction in DLAs decreases with increasing redshift.

This evolution is also apparent in DLA metallicities, which we use to gauge the abundance of heavy elements available to form tracer molecules. By scaling the H_2–CO & –HCO^+ column density ratios accordingly, we find:

- Although the GBT results offer a significant improvement over previous HCO^+ searches, the high redshifts ($z \gtrsim 2.5$) yield correspondingly large conversion ratios and excitation temperatures, i.e. $N_{\rm H_2} \gtrsim 10^{10} N_{\rm HCO^+}$, rendering high redshift searches sensitive only to molecular fractions of $f \sim 1$.
- Since many of the CO searches are performed in the 3-mm band, these are generally at much lower redshift. So in addition to the $z \gtrsim 1.7$ optical limits of electronic transitions, we can estimate lower redshift values from the rotational transitions. Although the statistics are small and the quality of the limits varied (i.e. some limits are only sensitive to $f \gtrsim 0.9$), assuming $N_{\rm H_2} \approx 10^{0.26 z_{\rm abs} + 4.75} N_{\rm CO}$, we obtain, for the general (non-H_2) DLA population, a 3σ limit of $f \lesssim 0.03$ at $z = 0.5$. For more diffuse clouds ($N_{\rm H_2} \approx 10^{0.26 z_{\rm abs} + 6} N_{\rm CO}$) this increases to $f \lesssim 0.2$.

Finally, we discuss the possibility of detecting CO absorption with the next generation of large radio telescopes in the context of the metallicity evolution model. Although the SKA will reach sensitivities of ~ 5 μJy after one hour of integration (c.f. ~ 300 μJy with ALMA), ALMA is the most likely to detect millimetre absorption in DLAs at low redshift due to its high frequency capabilities.

ACKNOWLEDGMENTS

We wish to thank Carl Bignell and Nario Kuno for their invaluable assistance in operating the Green Bank and Nobeyama 45-m telescopes, respectively. Also, the anonymous referee, Harvey Liszt and Max Pettini for their helpful comments, Chris Blake, Michael Burton, and Matthew Whiting for their input, as well as the John Templeton Foundation for supporting this work. SJC gratefully acknowledges receipt of a UNSW NS Global Fellowship and MTM is grateful to PPARC for support at the IoA under the observational rolling grant (PPA/G/O/2000/00039). This research has made use of the NASA/IPAC Extragalactic Database (NED) which is operated by the Jet Propulsion Laboratory, California Institute of Technology, under contract with the National Aeronautics and Space Administration.

[18] Note, however, that from Galactic studies, Liszt (2002) suggests that at very low metallicities H_2 will still via form slow gas-phase processes, giving minimum molecular fractions of $f \sim 10^{-8} - 10^{-7}$. This suggests that current DLA molecular fraction measurements may be close to the minimum possible value (see Ledoux et al. 2003; Reimers et al. 2003).

[19] Although Curran et al. (2004a) discuss the possibility of detecting low redshift OH 18-cm lines in DLAs with this telescope.

REFERENCES

Black J. H., Chaffee F. H., Foltz C. B., 1987, ApJ, 317, 442
Briggs F. H., Wolfe A. M., Liszt H. S., Davis M. M., Turner K. L., 1989, ApJ, 341, 650
Chaffee F. H., Black J. H., Foltz C. B., 1988, ApJ, 335, 584
Chandra S., Kegel W. H., Roy R. J. L., Hertenstein T., 1995, A&AS, 114, 175
Chandra S., Maheshwari V. U., Sharma A. K., 1996, A&AS, 117, 557
Combes F. Wiklind T., 1998, ESO Messenger, 91, 29
Curran S. J., Darling J. K., Kanekar N., 2004a, in Carilli C. L. et al., eds, Astrophysics with the Square Kilometer Array, Elsevier, in preparation
Curran S. J., Murphy M. . T., Pihlström Y. M., Purcell C. R., Webb, J. K. Kanekar, N., 2004b, MNRAS, in preparation
Curran S. J., Murphy M. T., Webb J. K., Pihlström Y. M., 2003, MNRAS, 340, 139
Curran S. J., Murphy M. T., Webb J. K., Rantakyrö F., Johansson L. E. B., Nikolić S., 2002a, A&A, 394, 763
Curran S. J., Webb J. K., Murphy M. T., Bandiera R., Corbelli E., Flambaum V. V., 2002b, PASA, 19, 455
Curran S. J., Webb J. K., Murphy M. T., Carswell R. F. 2004c, MNRAS, submitted (astro-ph/0311357)
Curran S. J., Webb J. K., Murphy M. T., Kuno N., 2004d, in Millar T. J., ed, ASP Conf. Ser., The Astrochemistry of External Galaxies, San Francisco, in press (astro-ph/0310589)
Drinkwater M. J., Webb J. K., Barrow J. D., Flambaum V. V., 1998, MNRAS, 295, 457
Ellison S. L., Pettini M., Steidel C. C., Shapley A. E., 2001, ApJ, 549, 770
Ellison S. L., Yan L., Hook I. M., Pettini M., Wall J. V., Shaver P. 2001, A&A, 379, 393
Ge J., Bechtold J., Walker C., Black J. H., 1997, ApJ, 486, 727
Kanekar N., Chengalur J. N., 2003, A&A, 399, 857
Kovalev Y. Y., Nizhelsky N. A., Kovalev Y. A., Berlin A. B., Zhekanis G. V., Mingaliev M. G., Bogdantsov A. V., 1999, A&AS, 139, 545
Kulkarni V. P., Fall S. M., 2002, ApJ, 580, 732
Lanzetta K. M., Wolfe A. M., Turnshek D. A., Lu L., McMahon R. G., Hazard C., 1991, ApJS, 77, 1
Ledoux C., Petitjean P., Srianand R., 2003, MNRAS, 346, 209
Liszt H., 2002, A&A, 389, 393
Liszt H., Lucas R., 2000a, A&A, 355, 333
Liszt H. S., Lucas R., 2000b, A&A, 355, 333
Lovas F. J., 1992, J. Phys. Chem. Ref. Data, 21, 181
Lu L., Sargent W. L. W., Barlow T. A., 1999, in Carilli C., Radford S. Menton K., Langston G., eds, ASP Conf. Ser. Vol. 156, Highly Redshifted Radio Lines, San Francisco, p. 132
Lu L., Sargent W. L. W., Barlow T. A., Churchill C. W., Vogt S. S., 1996, ApJS, 107, 475
Murphy M. T., Webb J. K., Flambaum V. V., Drinkwater M. J., Combes F., Wiklind T., 2001, MNRAS, 327, 1244
Péroux C., Storrie-Lombardi L. J., McMahon R. G., Irwin M., Hook I. M., 2001, AJ, 121, 1799
Petitjean P., Srianand R., Ledoux C., 2002, MNRAS, 332, 383

Pickett H. M., Poynter R. L., Cohen E. A., Delitsky M. L., Pearson J. C., Müller H. S. P., 1998, J. Quant. Spectrosc. Radiat. Transfer, 60, 883
Prochaska J. X., Gawiser E., Wolfe A. M., Castro S., Djorgovski S. G. 2003, ApJ, 595, L9
Rantakyrö F., Curran S. J., Murphy M. T., Staveley-Smith L., Webb J. K., 2004, MNRAS, in preparation
Rao S. M., Turnshek D. A., 2000, ApJS, 130, 1
Reimers D., Baade R., Quast R., Levshakov S. A., 2003, A&A, 410, 785
Rohlfs K., Wilson T. L., 2000, Tools of Radio Astronomy, Springer-Verlag, Berlin
Savage B. D., Sembach K. R., 1996, Ann. Rev. Astr. Ap., 34, 279
Steppe H., Jeyakumar S., Saikia D. J., Salter C. J., 1995, A&AS, 113, 409
Storrie-Lombardi L. J., Wolfe A. M., 2000, ApJ, 543, 552
Takahara F., Nakai N., Briggs F. H., Wolfe A. M., Liszt H. S. 1987, PASJ, 39, 933
Takahara F., Sofue Y., Inoue M., Nakai N., Tabara H., Kato T., 1984, PASJ, 36, 387
Teräsranta et al., 1998, A&AS, 132, 305
Tornikoski M., Lainela M., Valtaoja E., 2000, AJ, 120, 2278
Tsuboi M., Nakai N., 1991, PASJ, 43, L65
Turnshek D. A., Rao S. M., Ptak A. F., Griffiths R. E., Monier E. M., 2003, ApJ, 590, 730
Turnshek D. A., Wolfe A. M., Lanzetta K. M., Briggs F. H., Cohen R. D., Foltz C. B., Smith H. E., Wilkes B. J., 1989, ApJ, 344, 567
White R. L., Kinney A. L., Becker R. H., 1993, ApJ, 407, 456
Wiklind T., Combes F., 1994, A&A, 286, L9
Wiklind T., Combes F., 1995, A&A, 299, 382
Wiklind T., Combes F., 1996a, Nat, 379, 139
Wiklind T., Combes F., 1996b, A&A, 315, 86
Wiklind T., Combes F., 1996c, in Shaver P. A., Science with Large Millimetre Arrays, Proceedings of the ESO-IRAM-NFRA-Onsala Workshop, Springer-Verlag, Berlin, p. 86
Wiklind T., Combes F., 1997, A&A, 328, 48
Wiklind T., Combes F., 1998, ApJ, 500, 129
Wiklind T., Combes F., 1999, in Carilli, C., Radford, S. Menton, K., Langston, G., eds, ASP Conf. Ser. Vol. 156, Highly Redshifted Radio Lines, San Francisco, p. 202
Wolfe A. M., Lanzetta K. M., Foltz C. B., Chaffee F. H., 1995, ApJ, 454, 698

This paper has been typeset from a TEX/ LATEX file prepared by the author.